

Dynamics of Photoinduced Charge Separation on the Surface of Dihexadecylphosphate Vesicles

Rafail F. Khairutdinov[†] and James K. Hurst*

Department of Chemistry, Washington State University, Pullman, Washington, 99164-4630

Received: April 14, 1998; In Final Form: June 3, 1998

One-electron oxidation of triplet-photoexcited [5,10,15,20-tetrakis(*N*-methylpyridinium-4-yl)porphinato]zinc(II) (³ZnTMPyP⁴⁺) by *N*-alkyl-4-cyanopyridinium (C_{*n*}CP⁺) ions on an anionic dihexadecylphosphate (DHP) vesicle surface was studied by transient spectrophotometry. Surface rate constants for both oxidative quenching and charge recombination between the photoproducts, ZnTMPyP⁵⁺ and C_{*n*}CP⁰, were insensitive to the alkyl chain length of the electron acceptor over the range *n* = 6–16 carbon atoms, suggesting that the rate was determined primarily by the lateral mobility of the metalloporphyrin. Interfacial reductive quenching of DHP vesicle-bound ³ZnTMPyP⁴⁺ to ZnTMPyP³⁺ by dithiothreitol was 10³-fold slower than the corresponding reaction in homogeneous solution, an effect that was attributed to stabilization of the more highly charged tetracation by the anionic interface. The C_{*n*}CP⁰ radicals functioned as electron carriers to mediate photoinitiated transmembrane reduction of Co(bpy)₃³⁺ by dithiothreitol; rate constants for transmembrane C_{*n*}CP⁰ diffusion, evaluated from the quantum yields for Co(bpy)₃³⁺ reduction, were also insensitive to the alkyl chain length and had characteristic times of ~3 × 10⁻² s. These values were nearly identical to those obtained for the same reaction measured in another photoreactive system where the C_{*n*}CP⁰ radicals were generated in the bulk aqueous phase, rather than on the membrane surface. The quantum efficiency for transmembrane redox was relatively low, primarily because charge recombination of the photoredox products on the vesicle surface was rapid relative to either transmembrane diffusion of C_{*n*}CP⁰ or interfacial reduction of ZnTMPyP⁵⁺ by dithiothreitol.

Introduction

The topographic location of reactants within microphase-organized chemical systems can dramatically influence their reactivity characteristics.¹ For example, oxidative quenching of the excited triplet [5,10,15,20-tetrakis(4-sulfonatophenyl)porphinato]zinc(II) (³ZnTPPS⁴⁻) ion by viologens (e.g., *N,N'*-dimethyl-4,4'-bipyridinium, MV²⁺) leads to formation of long-lived redox products when the viologens are adsorbed to anionic dihexadecylphosphate (DHP) vesicles.² Photoproduct yields, which are exceptionally high (*ϕ* ≤ 0.7), are markedly decreased when the vesicles are absent, primarily because the zinc porphyrin and viologens undergo extensive ion-pairing leading to static quenching of the photoexcited ion. Thus, in the presence of vesicles, the viologen preferentially adsorbs to the anionic aqueous–organic interface, minimizing porphyrin–viologen association; although the ³ZnTPPS⁴⁻ ion is repelled from the interface, its lifetime is sufficiently long that oxidative quenching is still efficient. Furthermore, charge recombination between the aqueous ZnTPPS³⁻ π -cation and membrane-bound MV⁺ radical cation is retarded by the same electrostatic barrier that impedes the forward reaction, increasing the product lifetimes. In contrast, when ZnTPPS⁴⁻ is replaced by ZnTMPyP⁴⁺ ([5,10,15,20-tetrakis(*N*-methylpyridinium-4-yl)porphinato]zinc(II)), a cationic analogue with similar photophysical properties that strongly binds to DHP vesicles, photoyields are markedly diminished in the vesicle suspensions compared to the corresponding reaction in solution.³ Although these reac-

tions have been less intensively studied, this reduction in overall yield is thought to arise, at least in part, because rates of dissipative charge recombination and other cross-reactions are increased when the reactants are confined in close proximity on the vesicle surface.

The dynamical behavior of a very similar DHP vesicle-organized system utilizing ZnTPPS⁴⁻ as photosensitizer and a series of *N*-alkylcyanopyridinium (C_{*n*}CP⁺) ions as oxidative quenchers has recently been reported.⁴ The complete system contained electron donors in the bulk aqueous phase and electron acceptors in the internal aqueous phase, allowing transmembrane charge separation to also be observed. A comparative study utilizing ZnTMPyP⁴⁺ as photosensitizer (Figure 1) is presented herein; the study permits an unprecedented opportunity to compare the effects of photosensitizer location upon each of the elementary reaction steps in vesicle-organized assemblies.

Experimental Section

Materials. *N*-Alkyl-4-cyanopyridinium ions were synthesized from 4-cyanopyridine and an appropriate alkyl halide as described elsewhere.⁴ Dihexadecylphosphate small unilamellar vesicles, including those containing Co(bpy)₃³⁺ in their inner aqueous phase, were prepared and characterized as previously described.⁴ For all experiments, vesicles were formed from suspensions containing 4.4 mg/mL DHP, giving a final vesicle concentration of 2 μ M. The alkylpyridinium ions and ZnTMPyP⁴⁺ were added to the preformed vesicle suspensions as required to give the desired final reaction conditions. The suspensions were then deoxygenated by bubbling with purified Ar, following which portions of deoxygenated solutions con-

[†]Visiting scientist from the N. N. Semenov Institute of Chemical Physics.

*Correspondence should be addressed to this author. E-mail: hurst@wsu.edu. Fax: (509) 335-8867.

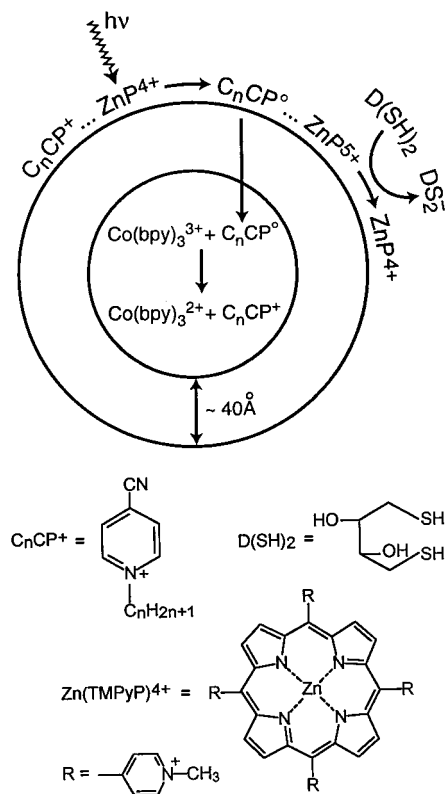


Figure 1. General reaction scheme for C_nCP^+ -mediated photoinduced charge transfer. Positively charged porphyrins and alkylpyridines are adsorbed onto the negatively charged DHP vesicles.

taining dithiothreitol ($D(SH)_2$) were added anaerobically using syringe-transfer techniques. Fresh stock solutions of dithiothreitol were prepared prior to each set of experiments. The complete system (Figure 1) was highly photoreactive; consequently, suspensions containing $D(SH)_2$ were protected from photodegradation by working in a minimal red light environment. All experiments were made in 20 mM Tris chloride, pH 8.0, at ambient temperature. All reagent solutions were prepared using water purified with a Milli-Q system.

Continuous and Laser Pulse Photolysis. The equipment used for both the continuous photolysis studies and the transient-kinetic measurements has been previously described, as have the general experimental procedures employed.⁴ For the current continuous photolysis studies, the procedures were modified as follows: to provide a wavelength appropriate for absorption into the $ZnTMPyP^{4+}$ Soret band, a 450 nm interference filter was placed between the excitation light source and sample compartment, and to minimize photodegradation by the analyzing light of the diode array spectrophotometer, a $ZnTMPyP^{4+}$ solution with an absorbance of 1.0 at its Soret band maximum was placed as a filter in the sample compartment of the spectrophotometer between the light source and the reaction cell. Reduction of $Co(bpy)_3^{3+}$ was monitored spectrophotometrically at 320 nm using $\Delta\epsilon_{320} = 2.85 \times 10^4 \text{ M}^{-1} \text{ cm}^{-1}$ for the $Co(bpy)_3^{3+}-Co(bpy)_3^{2+}$ difference extinction coefficient.⁵ Absolute quantum yields were determined at light intensities of $(2-8) \times 10^{-9}$ einstein/s; the portion of energy absorbed by the photosensitizer was determined by comparing transmittances of solutions with and without added $ZnTMPyP^{4+}$.

Absorption spectra and decay kinetics of reaction intermediates were measured by laser flash photolysis using the second harmonic (532 nm) from a Nd:YAG laser as the excitation source. Ultrafiltration studies using centrifugal microconcentrators⁴ indicated that the extent of $ZnTMPyP^{4+}$ binding to the

TABLE 1: Rate Constant Summary

C_nCP^+ (n)	$10^{-6}k_q (\text{M}^{-1} \text{s}^{-1})^a$		$10^{11} k_q^s (\text{cm}^2 \text{s}^{-1})^b$	$10^8 k_t^s (\text{cm}^2 \text{s}^{-1})^a$	$10^2 \tau_v (\text{s})^c$
	H ₂ O	vesicle			
1	6.2	0.12	9.5		
6	4.9	1.6	9.3	0.9	2.3
8	5.8	1.9	9.0	0.8	1.6
10	5.9	2.0	8.3	1.3	3.6
12	5.4	2.2	8.8	1.2	5
14		~1.7	~6.8	~1.4	>5
16		~2.5	~10	~1.8	>5

^a $\pm 20\%$. ^b $\pm 30\%$. ^c $\pm 50\%$.

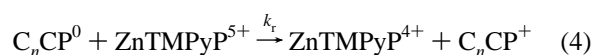
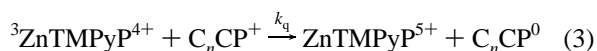
vesicles exceeded 95% under the experimental conditions. Vesicle binding caused the $^3ZnTMPyP^{4+}-ZnTMPyP^{4+}$ difference absorption maximum to shift from 470 nm to 480 nm; a difference extinction coefficient of $\Delta\epsilon_{480} = 6.4 \times 10^4 \text{ M}^{-1} \text{ cm}^{-1}$ was determined from the maximal absorbance change at 480 nm following a laser flash whose intensity was calibrated by ferrioxalate actinometry,⁶ assuming that $\phi = 0.90$ for the quantum yield for $^3ZnTMPyP^{4+}$ formation.⁷

Results and Discussion

Oxidative Quenching of $^3ZnTMPyP^{4+}$ by C_nCP^+ Ions.

Earlier studies had shown that the dynamics of $^3ZnTMPyP^{4+}$ decay on DHP vesicle surfaces was quite complicated, proceeding by as many as three kinetically distinguishable pathways.³ The present studies were performed using low $ZnTMPyP^{4+}$ /vesicle ratios, such that on average no more than one porphyrin was bound to each vesicle. With these constraints, the $^3ZnTMPyP^{4+}$ decay (reaction 2) followed simple first-order kinetics with a characteristic time $\tau = 1.96 \times 10^{-3} \text{ s}$.⁸

For both aqueous solutions and DHP vesicle suspensions, addition of C_nCP^+ ions caused the $^3ZnTMPyP^{4+}$ decay rate to increase; transient kinetic spectroscopy revealed sequential formation and decay of the $ZnTMPyP^{5+}$ π -cation radical,⁷ indicating that deactivation involved oxidative quenching of the photoexcited triplet by C_nCP^+ followed by charge recombination. The initial $^3ZnTMPyP^{4+}$ yield following laser flash excitation was independent of the identities or concentrations of C_nCP^+ , indicating that static quenching by $^3ZnTMPyP^{4+}-C_nCP^+$ aggregates was negligible. The reaction cycle



appeared to be fully reversible, since no changes were detected in the transient absorption spectrum, intermediate decay rate, or ground-state absorption spectrum of the system after exposure to more than 100 laser excitations.

To minimize potential complications arising from triplet-triplet annihilation reactions,^{4,9} transient kinetics studies were made using energies less than 100 mJ/pulse. Reactions were monitored at 480 and 700 nm, which correspond to the absorption maxima for $^3ZnTMPyP^{4+}$ and $ZnTMPyP^{5+}$, respectively.^{10,11} Bimolecular rate constants (k_q) for quenching by the various C_nCP^+ ions in homogeneous solution, determined from the concentration dependencies of the measured rate constant for $^3ZnTMPyP^{4+}$ decay, are given in Table 1; within experi-

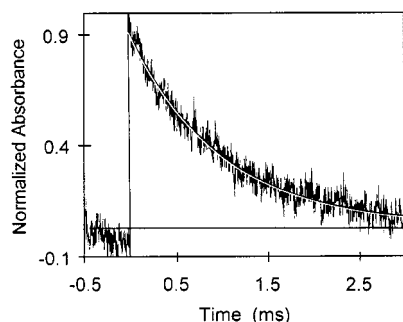


Figure 2. Absorbance changes at 480 nm following 20 mJ/pulse laser flash excitation of a deoxygenated 2 μ M suspension of DHP vesicles containing 2 μ M ZnTMPyP⁴⁺ and 400 μ M C₁₀CP⁺. The solid line is an exponential fit to the data with $k = 1.1 \times 10^3 \text{ s}^{-1}$.

mental uncertainty, the constants are independent of the quencher alkyl chain length, indicating that the inherent reactivities of the C_nCP⁺ ions are nearly identical. The values for k_q are 3 orders of magnitude lower than for the corresponding reactions with ³ZnTPPS⁴⁻, which are nearly diffusion controlled.⁴ Although charge repulsion may contribute to the slower rate of oxidative quenching of ³ZnTMPyP⁴⁺, the major effect is undoubtedly the unfavorable driving force for electron transfer. Reported standard reduction potentials are $E^\circ(\text{ZnTMPyP}^{5+}/\text{ZnTMPyP}^{4+}) = -0.45 \text{ V}^7$ and $E^\circ(\text{C}_1\text{CP}^{+/0}) = -0.65 \text{ V}^{12}$ so that the overall reaction is endergonic by -0.2 V . (All potentials cited are referenced to NHE.)

In DHP vesicular suspensions, both the positively charged porphyrin and C_nCP⁺ with $n \geq 6$ are located primarily on the surface of anionic DHP vesicles (Figure 1);⁴ consequently, reaction between them is restricted to diffusional motion on the surface of the vesicle. At long times, the kinetics of quenching of excited molecules by acceptors on the surface of a sphere should be approximated by a simple exponential law.¹³ We use this exponential approximation to quantitatively analyze the quenching dynamics of DHP-bound ³ZnTMPyP⁴⁺ by C_nCP⁺ and present in the Appendix a mathematical justification for its use.

A typical ³ZnTMPyP⁴⁺ decay profile in DHP vesicular suspensions containing C_nCP⁺ is shown in Figure 2. Rate constants (k_q) evaluated from an exponential fit of the ³-ZnTMPyP⁴⁺ decay profile as a function of C_nCP⁺ concentration are summarized in Table 1. For these calculations, the reactant C_nCP⁺ concentrations were assumed to be equal to the total added concentrations, i.e., were not corrected for only partial binding to the DHP vesicles. In this sense, the measured k_q values are apparent rate constants.

Unlike the reactions in homogeneous solution, k_q values for the reactions in DHP vesicles increased progressively with increasing chain length (Table 1). This behavior indicates that the vesicle-bound fractions of C_nCP⁺ were more reactive toward ³ZnTMPyP⁴⁺ than were the fractions in the bulk aqueous phase. Assuming that the unbound quencher is totally unreactive, the actual rate constant between vesicle-bound reactants ($(k_q)_v$) is related to the experimentally determined rate constant (k_q) by

$$k_q = F(k_q)_v \quad (5)$$

where F is the fraction of C_nCP⁺ that is bound. This fraction has been previously determined for the conditions of these experiments.⁴ Calculated $((k_q)_v)$ and experimental (k_q) rate constants are compared in Figure 3. Interestingly, the values for $(k_q)_v$ are nearly independent of quencher alkyl chain length. Assuming that reaction is indeed confined to the vesicles, surface

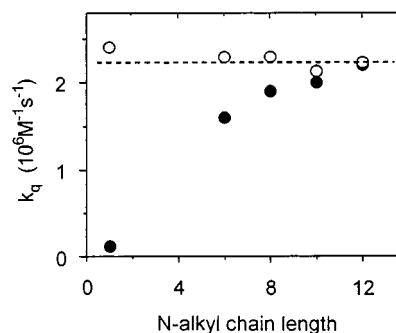


Figure 3. Dependence of the rate constant for oxidative quenching of ³ZnTMPyP⁴⁺ by C₁₀CP⁺ upon the N-alkyl chain length in DHP vesicular suspensions. Solid circles: experimental rate constants (k_q). Open circles: rate constants $((k_q)_v)$ calculated from eq 5.

quenching rate constants can be calculated from the following equation:

$$k_q^s = \frac{k_q c_v 4\pi R^2}{F} \quad (6)$$

where R is the DHP vesicle radius and c_v is the vesicle concentration. Values for k_q^s , calculated assuming $R = 12.5 \text{ nm}$,¹⁴ are listed in Table 1.

The kinetics of disappearance of DHP-bound ZnTMPyP⁵⁺ were studied at 700 nm. Because both ³ZnTMPyP⁴⁺ and ZnTMPyP⁵⁺ absorb at this wavelength, the following equation was used to describe the temporal changes:

$$A_{700}(t) = A_0 \exp\left(-k_q^s c_a^s t - \frac{t}{\tau}\right) + A_1 \left[1 - \exp\left(-k_q^s c_a^s t - \frac{t}{\tau}\right)\right] \exp(-k_r^s c_o^s t) \quad (7)$$

The first term on the right side of eq 7 corresponds to absorption by ³ZnTMPyP⁴⁺ and the second term to absorption by ZnTMPyP⁵⁺; A_0 and A_1 are constants; c_a^s and c_o^s are C_nCP⁺ and C_n-CP⁰ concentrations on the vesicle surface, respectively; and k_r^s is the rate constant of reaction 4 on the vesicle surface. In the second term, the expression in square brackets describes accumulation of ZnTMPyP⁵⁺ by oxidative quenching of ³-ZnTMPyP⁴⁺, and the following expression describes ZnTMPyP⁵⁺ decay via recombination with C_nCP⁰. We did not get reliable data on k_r for C₁CP⁺ because it binds DHP vesicles only very weakly ($F = 0.05$).⁴ Rate constants k_r^s for all other C_nCP⁺ ions are $\sim 10^{-8} \text{ cm}^2 \text{ s}^{-1}$; they are summarized in Table 1. The use of an exponential rate law to describe reaction 4 on vesicle surfaces is also justified in the Appendix.

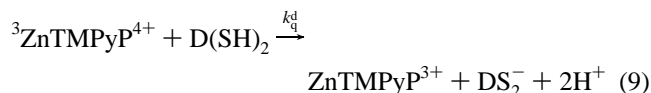
In homogeneous solution, reaction 4 is exergonic by $\Delta E = 1.8 \text{ V}$;^{7,12} assuming that the corresponding reaction on the vesicle surface is diffusion controlled, it follows (Appendix) that

$$k_r^s \approx 0.1667 \times 4\pi D \quad (8)$$

where D is the sum of the ZnTMPyP⁵⁺ and C_nCP⁰ surface diffusion coefficients. Using the above value of k_r^s , one obtains $D \approx 5 \times 10^{-9} \text{ cm}^2 \text{ s}^{-1}$. Note that this treatment may overestimate D because the initial distribution of ZnTMPyP⁵⁺ and C_nCP⁰ formed by oxidative quenching is nonrandom; consequently, the kinetics of their recombination may be faster than if randomly distributed on the vesicle surface.¹⁵⁻¹⁷

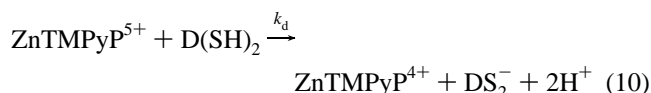
Reactions with Electron Donors. Standard potentials for one-electron reduction of the triplet photoexcited zinc porphyrin and the dithiothreitol disulfide anion radical are $E^\circ(\text{ZnTMPyP}^{4+}/$

$\text{ZnTMPyP}^{3+} = 0.78 \text{ V}^7$ and $E^\circ(\text{DS}_2^-, 2\text{H}^+/\text{D}(\text{SH})_2) = 1.73 \text{ V}^{18}$. Consequently, the reaction



is nearly isoenergetic ($\Delta E = -0.01 \text{ V}$) in aqueous solution at pH 8. Reductive quenching by $\text{D}(\text{SH})_2$ was observed by laser flash photolysis; the rate constants (k_d) determined from the transient decay kinetics at 480 nm were $3.3 \times 10^8 \text{ M}^{-1} \text{ s}^{-1}$ for the aqueous reaction and $2 \times 10^5 \text{ M}^{-1} \text{ s}^{-1}$ for the DHP vesicle-bound porphyrin. The rate retardation by vesicles may reflect the influence of the anionic surface upon the thermodynamic potential for porphyrin reduction. Conceptually, binding in a highly anionic microenvironment should make reduction less favorable; this effect has been demonstrated for vesicle-bound viologens, for which shifts of $\approx -100 \text{ mV}$ were measured between neutral (zwitterionic) and anionic surfaces.¹⁹ Thus, reaction 9 on the vesicle surface is probably energetically unfavorable.

The rate of reduction of ZnTMPyP^{5+} produced by oxidative quenching by C_nCP^+ in aqueous and vesicular solutions increased upon addition of $\text{D}(\text{SH})_2$. Based upon reported reduction potentials for ZnTMPyP^{5+} ($E^\circ(\text{ZnTMPyP}^{5+/4+}) = 1.18 \text{ V}^7$) and DS_2^- , the reaction



is energetically favorable by $\Delta E = 0.39 \text{ V}$ at pH 8. The bimolecular rate constants (k_d), estimated from the transient decay kinetics at 700 nm, were $6 \times 10^8 \text{ M}^{-1} \text{ s}^{-1}$ in aqueous solution and $4 \times 10^5 \text{ M}^{-1} \text{ s}^{-1}$ in vesicle suspensions. As for reaction 9, the lower rate constant may reflect stabilization of ZnTMPyP^{5+} by the anionic surface.

Quantum Yields for Transmembrane Reduction of $\text{Co}(\text{bpy})_3^{3+}$. In this study, we found that photoexcitation of the complete system (Figure 1) resulted in reduction of entrapped $\text{Co}(\text{bpy})_3^{3+}$ to $\text{Co}(\text{bpy})_3^{2+}$, although reduction was insignificant when any of the components were deleted. In an earlier study using ZnTPPS^{4-} as photosensitizer, we had found that reduction of internal $\text{Co}(\text{bpy})_3^{3+}$ was accompanied by 1:1 net stoichiometric uptake of C_nCP^+ , establishing that C_nCP^0 acted as the mobile electron carrier in that system.⁴ The analogous transmembrane redox step for this system is



where the notation (...) _i refers to species located within the vesicle. Since $E^\circ(\text{Co}(\text{bpy})_3^{3+/2+}) = 0.35 \text{ V}$,²⁰ the driving force for these reactions is large ($\Delta E \approx 1.0 \text{ V}$). Reaction between $\text{Co}(\text{bpy})_3^{3+}$ and C_nCP^0 in homogeneous solution is rapid; the corresponding membrane-separated reaction is rate-limited by transmembrane diffusion of C_nCP^0 .

Reaction 11 could not be studied directly by transient spectrophotometry in this system because formation of C_nCP^0 was too inefficient to allow accumulation of detectable concentrations in the laser flash. However, the characteristic time (τ_v) can be evaluated from the quantum yield data for $\text{Co}(\text{bpy})_3^{3+}$ reduction measured by continuous photolysis. These quantum yields were dependent upon the identity and concentration of C_nCP^+ , as well as the $\text{D}(\text{SH})_2$ concentration. Typical dependencies are illustrated in Figures 4 and 5 for C_{10}CP^+ as

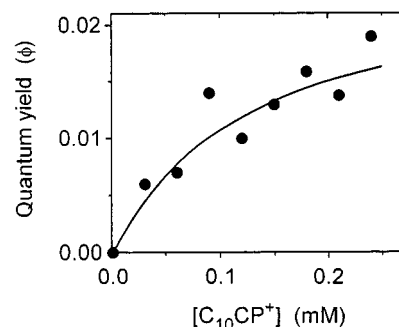


Figure 4. Dependence of the quantum yield for C_{10}CP^+ -mediated $\text{Co}(\text{bpy})_3^{3+}$ reduction to $\text{Co}(\text{bpy})_3^{2+}$ upon the C_{10}CP^+ concentration. Conditions: [vesicles] = $2 \mu\text{M}$; $[\text{ZnTMPyP}^{4+}] = 2 \mu\text{M}$; $[\text{D}(\text{SH})_2] = 150 \mu\text{M}$. Data points are indicated by the solid circles; the line is the fit to eq 12 with $\tau_v = 3.6 \times 10^{-2} \text{ s}$ and other constants as given in the text.

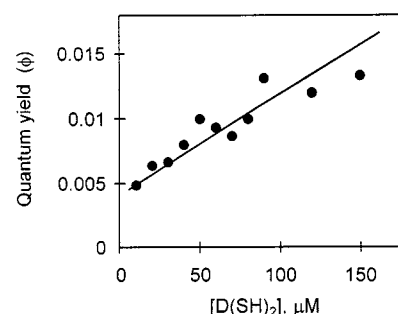


Figure 5. Dependence of the quantum yield for C_{10}CP^+ -mediated $\text{Co}(\text{bpy})_3^{3+}$ reduction to $\text{Co}(\text{bpy})_3^{2+}$ upon the $\text{D}(\text{SH})_2$ concentration. Conditions: [vesicles] = $2 \mu\text{M}$; $[\text{ZnTMPyP}^{4+}] = 2 \mu\text{M}$; $[\text{C}_{10}\text{CP}^+] = 90 \mu\text{M}$, 23°C . Data points are indicated by the solid circles; the line is the fit to eq 12 with $\tau_v = 3.6 \times 10^{-2} \text{ s}$ and other constants as given in the text.

the electron carrier; under the experimental conditions, the reactions proceeded almost exclusively by oxidative quenching.

The quantum yield data were analyzed quantitatively by considering reactions 1–4, 10, and 11. The DS_2^- radical formed in reaction 10 is both strongly oxidizing and reducing ($E^\circ(\text{DS}_2^{0/-}) = -1.60 \text{ V}$)¹⁸ and could react with C_nCP^+ to generate additional C_nCP^0 ($\Delta E = 0.95 \text{ V}$) or reduce ZnTMPyP^{5+} to ZnTMPyP^{4+} ($\Delta E = 2.8 \text{ V}$), which are reactions that would increase the overall quantum yield. Alternatively, DS_2^- could engage in a dissipative cross-reaction with C_nCP^0 ($\Delta E = 1.4 \text{ V}$, pH 8), thereby reducing the overall quantum yield. However, since all of these species are membrane-bound and the DS_2^- radical is a hydrophilic anion that should be strongly repelled from the vesicle surface, we assume that the primary reaction for its disappearance is disproportionation in the bulk aqueous phase to DS_2 and $\text{D}(\text{SH})_2$, a reaction that is also strongly exergonic ($\Delta E = 2.4 \text{ V}$, pH 8). Conversely, the C_nCP^0 radicals formed in reaction 3 are hydrophobic and are expected to remain bound to the DHP vesicle until either undergoing charge recombination with ZnTMPyP^{5+} (reaction 4) or reducing entrapped $\text{Co}(\text{bpy})_3^{3+}$ (reaction 11). With these constraints, and assuming that each C_nCP^0 that traverses the bilayer reduces a $\text{Co}(\text{bpy})_3^{3+}$ to $\text{Co}(\text{bpy})_3^{2+}$, the overall quantum yield for $\text{Co}(\text{bpy})_3^{3+}$ reduction (ϕ) is given by

$$\phi = \varphi \frac{k_q^s c_s}{k_q^s c_s + \tau^{-1}} \phi_{cs} \frac{k_d c_d + \tau_v^{-1}}{k_d c_d + \tau_v^{-1} + k_r} \quad (12)$$

where φ is the quantum yield for $^3\text{ZnTMPyP}^{4+}$ generation, the second term on the right side of eq 12 is the fraction of

$^3\text{ZnTMPyP}^{4+}$ that is oxidized to generate C_nCP^0 , ϕ_{cs} is the fraction of C_nCP^0 in the geminate pair that escapes cage recombination with ZnTMPyP^{5+} , the fourth term is the fraction of the rest of the C_nCP^0 that escapes bulk recombination with ZnTMPyP^{5+} to reduce $\text{Co}(\text{bpy})_3^{3+}$, and c_d is the bulk concentration of $\text{D}(\text{SH})_2$. Equation 12 is based on the assumption that C_nCP^0 and ZnTMPyP^{5+} are created in contact and then react with each other during their random walk.

From eq 12 one has for the relative quantum yield

$$\frac{\phi}{\phi_0} = \frac{(k_d c_d + \tau_v^{-1})(1 + k_t \tau_v)}{k_d c_d + \tau_v^{-1} + k_t} \quad (13)$$

where ϕ_0 is the quantum yield for $\text{Co}(\text{bpy})_3^{3+}$ reduction to $\text{Co}(\text{bpy})_3^{2+}$ in the absence of $\text{D}(\text{SH})_2$.

The characteristic time for transmembrane diffusion of C_nCP^0 (τ_v) can be calculated from eq 13 because all of the other experimental variables have been determined. Best-fit values obtained over a range of medium conditions for each C_nCP^0 radical are summarized in Table 1. The values were remarkably similar for the radicals with alkyl chains containing 6–12 carbon atoms, with an overall average of $\tau_v \approx 3 \times 10^{-2}$ s; with $n = 14$ or 16, the accuracy of the quantum yield measurements was lower than for the other C_nCP^0 , and only a lower limit of $\tau_v > 5 \times 10^{-2}$ s could be set for these radicals.

General Comments. *Transmembrane Diffusion of C_nCP^0 .* The τ_v values calculated from the overall quantum yields agree well with previously measured relaxation times for reaction 11 in a different photoreaction system, for which $\tau_v = 2 \times 10^{-2}$ s.⁴ In that system, oxidative quenching of $^3\text{ZnTPPS}^{4-}$ by C_nCP^+ occurred in the bulk aqueous phase; $\text{Co}(\text{bpy})_3^{3+}$ ions in the inner aqueous compartment of DHP vesicles were reduced to $\text{Co}(\text{bpy})_3^{2+}$ by a unimolecular process which could be observed directly by transient spectrophotometry. The observation that nearly identical constants were obtained despite the differing locations of C_nCP^0 formation (aqueous phase vs vesicle surface) is consistent with a mechanism for reaction 11 involving rate-limiting transmembrane diffusion of strongly bound lipophilic radicals across the hydrocarbon phase of the membrane. Additionally, the agreement between τ_v values calculated from quantum yields for the $^3\text{ZnTMPyP}^{4+}$ -photosensitized reaction and the directly determined values from the $^3\text{ZnTPPS}^{4-}$ -photosensitized reaction supports the premises that were made in deriving eq 12, i.e., that individual reaction steps involving C_nCP^0 are confined to the vesicle and those involving DS_2^- occur in the bulk aqueous phase. Had the major decay pathways not been correctly identified, the calculated value for τ_v would have differed significantly from the experimental value. The transmembrane diffusion coefficients of C_nCP^0 , estimated from the Smoluchowski–Einstein equation ($D \approx l^2/\tau_v$, where $l \approx 4$ nm is the hydrocarbon bilayer width), are $\sim 10^{11} \text{ cm}^2 \text{ s}^{-1}$; this corresponds to permeability coefficients $P = l/\tau_v \approx 2 \times 10^{-5} \text{ cm/s}$.

Quantum Yields for Transmembrane Redox. The quantum yields for transmembrane reduction of $\text{Co}(\text{bpy})_3^{3+}$ are 50–100-fold lower for these reactions, where C_nCP^0 are generated by reaction with $^3\text{ZnTMPyP}^{4+}$ on the DHP vesicle surface, than for the corresponding reactions⁴ which are initiated by C_nCP^0 formation in the bulk aqueous phase by oxidative quenching of $^3\text{ZnTPPS}^{4-}$. This behavior parallels results of earlier studies described in the Introduction wherein photosensitized reduction of DHP vesicle-bound viologens occurred much more efficiently when the reactions occurred across the aqueous–organic interface than on the vesicle surface.^{2,3} In the present case,

examination of eq 12 reveals the origin of the low quantum yields for the surface-confined reaction. The fraction of $^3\text{ZnTMPyP}^{4+}$ that undergoes oxidative quenching (given by the second right-hand term) is 0.15–0.5 under the experimental conditions; however, the fraction of the C_nCP^0 formed that does not recombine with ZnTMPyP^{5+} (given by the third term) is only 0.02–0.04. Thus, the dominant factor limiting the quantum yield is the large rate constant for charge recombination on the vesicle surface (reaction 4) relative to either transmembrane diffusion of C_nCP^0 or interfacial reduction of ZnTMPyP^{5+} by $\text{D}(\text{SH})_2$.

Acknowledgment. Funding for this research was provided by the Division of Chemical Sciences, Office of Basic Energy Sciences, U.S. Department of Energy, under Grant DE-FG06-95ER14581.

Appendix

Monte Carlo simulations were made to justify the use of an exponential decay equation in analyzing the kinetics of $^3\text{ZnTMPyP}^{4+}$ disappearance on the vesicle surface. These simulations show that the decay kinetics can be approximated by a single exponential, the rate constant for which depends linearly upon the initial concentration of the electron acceptor and upon the reagent diffusion coefficient.

The vesicles were modeled as spheres with radii R . Electron donor and acceptor molecules were considered as circles with radii r_d and r_a , respectively, which were placed randomly on the sphere subject to the constraints that the point of contact was the center of the circle and no circles intersected. The initial state was prepared by randomly selecting some of donor molecules to be photoexcited. The numbers of donor molecules, excited donor molecules, and acceptors were varied from trial to trial in a manner such that their values averaged over all trials were fixed and equal to average number of donor molecules, excited donor molecules, or acceptors per sphere in the system.

After preparation of the initial state at $t = 0$, Monte Carlo moves were made at time intervals τ on each of the donor and acceptor molecules in the system. At every move, each molecule was permitted to shift randomly in any direction for a distance λ along the surface of the sphere. However, molecules were not allowed to leave the surface. The values of τ and λ changed randomly from one move to another in the intervals $0 - \tau_D$ and $0 - \lambda_D$, respectively. Each excited molecule decayed with an intrinsic lifetime of τ_0 . Any pair of excited donor and acceptor molecules was permitted to undergo electron transfer quenching at each Monte Carlo move with the probability w per unit time given by the equation^{21,22}

$$w = \nu \exp(-(r - d)/2a) \quad (\text{A1})$$

where ν is the frequency factor, a is the parameter that describes the decrease of quenching rate with distance r between interacting molecules, and d is the sum of the radii of the reactants. The final Monte Carlo decay curves were obtained by averaging results obtained from more than 10 000 individual trials. Different curves were obtained using the following ranges of experimental parameters: vesicle radius R , 10–20 nm; donor and acceptor radii, 0.2–0.5 nm; average number of acceptor molecules/sphere, 0.5–45; average number of donor molecules/sphere, 1.0; λ_D , 0.04–0.1 nm; τ_D , 10^{-7} – 10^{-10} s; a , 0.05–0.3 nm; ν , 10^9 – 10^{15} s^{-1} .

Typical logarithmic plots of calculated decay curves for excited donor molecules obtained with several average numbers

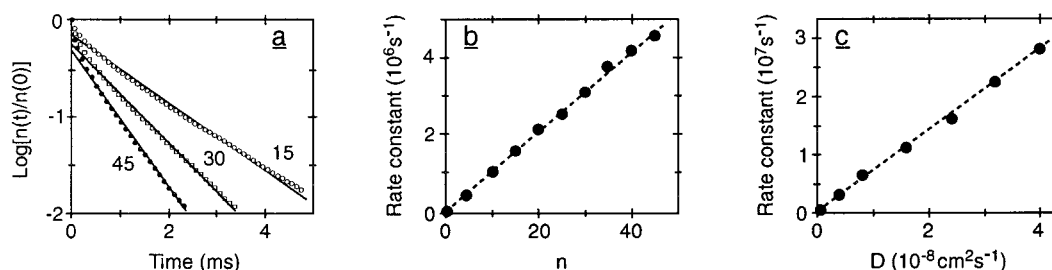


Figure 6. Monte Carlo calculations. Panel a: Decay curves for quenching of excited molecules on a sphere of radius $R = 12.5$ nm for three different average numbers of acceptor molecules (points) and the best-fit exponential approximations to these decays (lines). Parameters used in the calculations are $r_d = 0.5$ nm, $r_a = 0.3$ nm, $\nu = 10^{11}$ s $^{-1}$, $a = 0.1$ nm, $\tau_D = 10^{-7}$ s, $\lambda_D = 0.1$ nm; $\tau = 3.8 \times 10^{-3}$ s. The numbers given in the figure are the average number of acceptor molecules for the corresponding curves. Panel b: Dependence of the quenching rate constant on the average number of acceptor molecules on the surface of the sphere. Panel c: Dependence of the quenching rate constant on the surface diffusion constant.

of acceptor molecules/vesicle are given in Figure 6 (panel a); the near-linearity of these plots validates the use of a single-exponential decay law to describe the decay. The dependence of the apparent first-order rate constant is plotted against the acceptor concentration in Figure 6 (panel b), and the dependence of the rate constant on the surface diffusion constant of the reactants, defined as $D \approx \lambda_D^2/\tau_D$, is plotted in Figure 6 (panel c); in both cases, a linear dependence is demonstrated.

To justify the use of a single-exponential decay equation to analyze the kinetics of charge recombination (reaction 4), we examined the analytical solution for the kinetics of a diffusion-controlled reaction for a pair of particles on a spherical surface, which is expressed by the sum of exponentials:¹³

$$\frac{n(t)}{n(0)} = \sum_{i=1}^{\infty} c_i \exp\left(-\frac{t}{\tau_i}\right) \quad (\text{A2})$$

(Recall that, under our experimental conditions, on average less than one $^3\text{ZnTMPyP}^{4+}$ - C_{60}NP^0 pair is generated per vesicle.) In eq A2, the coefficients c_i and characteristic times τ_i can be numerically calculated for any given sizes of the sphere and the reagents.¹³ For our system, numerical calculations of the first five members of the series in eq A2 generate the following kinetic expression:

$$\begin{aligned} \frac{n(t)}{n(0)} = & 0.9720 \exp(-0.1667t/\tau_D) + \\ & 0.0163 \exp(-2.6091t/\tau_D) + 0.0051 \exp(-7.1817t/\tau_D) + \\ & 0.0019 \exp(-13.8640t/\tau_D) + 0.0015 \exp(-22.6491t/\tau_D) \end{aligned} \quad (\text{A3})$$

where the characteristic time τ_D is given by $\tau_D = R^2/D$. Clearly, the first term dominates the sum, indicating that the reaction is well-approximated by a single exponential.

References and Notes

- (1) Gratzel, M.; Kalyanasundaram, K. *Kinetics and Catalysis in Microheterogeneous Solutions*; Surfactant Science Series, Vol. 38; Marcel Dekker: New York, 1991.
- (2) Hurst, J. K.; Thompson, D. H. P.; Connolly, J. S. *J. Am. Chem. Soc.* **1987**, *109*, 507.
- (3) Hurst, J. K.; Lee, L. Y. C.; Gratzel, M. *J. Am. Chem. Soc.* **1983**, *105*, 7048.
- (4) Lymar, S. V.; Khairutdinov, R. F.; Soldatenkova, V. A.; Hurst, J. K. *J. Phys. Chem.* **1998**, *102*, 2811.
- (5) Lymar, S. V.; Hurst, J. K. *J. Phys. Chem.* **1994**, *98*, 989.
- (6) Hatchard, C. G.; Parker, C. A. *Proc. R. Soc., Ser. A* **1956**, 235, 518.
- (7) Kalyanasundaram, K.; Neumann-Spallart, M. *J. Phys. Chem.* **1982**, *86*, 5163.
- (8) The extent to which quenching by O_2 contributes to triplet decay is difficult to assess. Reported triplet lifetimes for ZnTMPyP^{4+} in aqueous solutions are typically $\tau \approx 1$ ms.⁷ Using a purging line constructed entirely of copper tubing and glass that incorporates commercial Cu^0 -based O_2 traps, we routinely obtain $\tau \approx 2$ ms. This behavior indicates that reaction with O_2 contributes to the decay, at least at the shorter lifetimes. Since the purging efficiency remains nearly constant throughout the measurements, any quenching by O_2 will not affect the values of rate constants determined for the other quenchers.
- (9) Assuming random binding characterized by a Poisson-type distribution, when the average number of ZnTMPyP^{4+} /vesicle = 1, 26% of the vesicles will contain two or more porphyrins.
- (10) Neta, P. *J. Phys. Chem.* **1981**, *85*, 3678.
- (11) Borgarello, E.; Kalyanasundaram, K.; Okuno, Y.; Gratzel, M. *Helv. Chim. Acta* **1981**, *64*, 1937.
- (12) Harriman, A.; Millward, G. R.; Neta, P.; Richoux, M. C.; Thomas, J. M. *J. Phys. Chem.* **1988**, *92*, 1286.
- (13) Sano, H.; Tachiya, M. *J. Chem. Phys.* **1981**, *75*, 2870.
- (14) Humphry-Baker, R.; Thompson, D. H.; Lei, Y.; Hope, M. J.; Hurst, J. K. *Langmuir* **1991**, *7*, 2592.
- (15) Dorfman, R. C.; Fayer, M. D. *J. Chem. Phys.* **1992**, *96*, 7410.
- (16) Burstein, A. I.; Krissinel, E.; Mikhelashvili, M. S. *J. Phys. Chem.* **1994**, *98*, 7319.
- (17) Mikhelashvili, M. S.; Michaeli, A. M. *J. Phys. Chem.* **1994**, *98*, 8114.
- (18) Surdhar, P. S.; Armstrong, D. A. *J. Phys. Chem.* **1987**, *91*, 6532.
- (19) Lei, Y.; Hurst, J. K. *J. Phys. Chem.* **1991**, *95*, 7918.
- (20) Farina, R.; Wilkins, R. G. *Inorg. Chem.* **1968**, *7*, 514.
- (21) Khairutdinov, R. F.; Serpone, N. *Prog. React. Kinet.* **1996**, *21*, 1.
- (22) Khairutdinov, R. F.; Zamaraev, K. I.; Zhdanov, V. P. *Electron Tunneling in Chemistry*; Elsevier: Amsterdam, 1989.